RSC Advances

PAPER

View Article Online
View Journal | View Issue

Cite this: *RSC Adv.*, 2023, **13**, 16789

Surface modification of mild steel using 4-carboxyphenyl diazonium in sulfuric and hydrochloric acids. A corrosion study†

Patrick Marcel Seumo Tchekwagep, *[ab] Goncagül Aksaray, [a] Murat Farsak[c] and Gülfeza Kardaş*[a]

Received 2nd March 2023
Accepted 22nd May 2023

DOI: 10.1039/d3ra01415k

rsc.li/rsc-advances

In this paper, the surface of mild steel is modified with 4-carboxyphenyl diazonium and subsequently, the corrosion behaviour of the modified surface is scrutinized in hydrochloric and sulfuric acid solutions. The diazonium salt was synthesized *in situ* either in 0.5 M HCl or 0.25 M H_2SO_4 through the reaction between 4-aminobenzoic acid and sodium nitrite. The surface of mild steel was modified with the obtained diazonium salt with or without the need for electrochemical assistance. Electrochemical impedance spectroscopy (EIS) measurements show that a spontaneously grafted mild steel surface has a better corrosion inhibition efficiency (86%) in 0.5 M HCl. Scanning electron microscopy reveals that the protective film formed on the surface of mild steel exposed to 0.5 M HCl containing the diazonium salt looks more consistent and uniform compared to the surface exposed to 0.25 M H_2SO_4. Optimized diazonium structure and the separation energy calculated using density functional theory correlate with the good corrosion inhibition obtained experimentally.

1. Introduction

Corrosion is a natural phenomenon leading to the deterioration of metals. From rusted iron to tarnished silver, corrosion is one of the great concerns of industry with a global cost estimated at around USD 2.5 trillion per year.[1] Additionally, many accidents ranging from plane crashes[2] to pipeline explosions[3] are associated with metal failure. Therefore, major sectors including the oil and gas industry, transportation, and infrastructure, spend millions of dollars on corrosion monitoring and maintenance activities yearly. It is important to mention that to date, there is still no foolproof solution which addresses corrosion drawbacks. This is mainly due to the inherent thermodynamic instability of metals. However, numerous studies have shown that corrosion can be retarded using corrosion inhibitors,[4,5] additives,[6,7] and coatings.[8,9]

Until recently, the chromium oxyhydroxide layer was widely exploited to slow down the corrosion rate. However, even though chromium(VI) compounds are effective, they are extremely hazardous being both carcinogen and hemolytic compounds, capable of causing kidney and liver failure.[10]

Nowadays scientists are devoted to research chemicals capable of inhibiting corrosion. Being corrosion an electrochemical reaction, strategies for engineering metals consist essentially to impede electrons or ions transport or to create a physical barrier for oxygen or water diffusion. Among chemicals, it is now well established that organic compounds containing polar functions with N, S or O atoms as well as conjugated double bonds or aromatic rings are good corrosion inhibitors.[4–6,11–14]

Given that aryl diazonium salts contain at least two N atoms and one aromatic ring, one can expect corrosion inhibition properties from these compounds. Screening the literature, few studies have been devoted to investigate application against corrosion of films produced *via* either electrografting or spontaneous grafting of diazonium salts on metal surfaces.[15–20] Adenier *et al.* have shown that electrochemical reduction of aryl diazonium salts on iron or mild and stainless steel permits a strong bonding of aryl groups on these surfaces.[15] The stable Fe–Aryl bond permits the formation of an organic layer providing a protection of the mild steel against corrosion. The authors claimed that even though thermodynamically diazonium salts can be spontaneously reduced at the metal surface, this reaction is slow to occur at a significant extend compared to an overpotential activation. In their work, Combellas *et al.* have chemically grafted on iron surfaces at open circuit potential different aryl diazonium salts in aqueous acidic solution without electrochemical assistance.[18] They have demonstrated

[a]*Chemistry Department, Faculty of Arts and Sciences, Çukurova University, 01330 Balcalı, Adana, Turkey. E-mail: 3omues@gmail.com; gulfeza@cu.edu.tr*

[b]*Analytical Chemistry Laboratory, Faculty of Science, University of Yaoundé 1, 812 Yaoundé, Cameroon*

[c]*Department of Battery Systems and Hydrogen Technologies, Osmaniye Korkut Ata University, Institute of Natural and Applied Science, Turkey*

† Electronic supplementary information (ESI) available. See DOI: https://doi.org/10.1039/d3ra01415k

the grafting of organic moieties without any adsorption of diazonium salts. Furthermore, they have provided evidence showing that spontaneous grafting in water is at least as efficient as electrochemical grafting. The film formed has a corrosion inhibition efficiency up to 73%, which can be significantly improved to 97% when the grafted metal is left in the corrosion medium in the presence of the diazonium salt. Berisha *et al.* have investigated a possible involvement of an adsorption step during the electrografting of two diazonium salts, namely 3,5-dimethylbenzene diazonium and 2,6-dimethylbenzene diazonium salts (3,5- and 2,6-DMBD, respectively), on the corrosion of iron.[19] If 3,5-DMBD has exhibited anticorrosive effect, on the other hand 2,6-DMBD did not show any inhibition effect. This was explained by the steric hindrance of the two methyl groups in α position of the radical in the case of 2,6-DMBD, and the absence of adsorption of this diazonium salt onto the iron surface. Therefore, they have concluded that besides the absence of grafting there was no physical adsorption of diazonium salts onto the iron surface.

The present work reports the synthesis and grafting of a simple aryl diazonium salt, prepared from 4-aminobenzoic acid, on mild steel surface in hydrochloric and sulfuric acid solutions. Furthermore, the effect of chlorides and sulfates on inhibition performances is discussed. Density functional calculation is complemented to provide a supplementary insight information needed for a better understanding.

2. Experimental

2.1. Materials and chemicals

Two mild steel (MS) samples containing 0.17% C, 0.045% S, 1.40% Mn, 0.009% N and remainder Fe were used in this study. The first sample was a cylindrical disc with 0.5 cm^2 surface area, which was used as the working electrode for electrochemical experiments. The second sample was a 1 × 1 × 0.1 cm^3 plate of MS, which was used for SEM-EDX and contact angle analysis.

Sulfuric acid 95% was purchased from VWR. Hydrochloric acid fuming 37%, 4-aminobenzoic acid and sodium nitrite were purchased from Merck. Double distilled water was used to prepare all solutions.

2.2. Preparation and characterization of diazonium salt of 4-aminobenzoic acid

50 mL of 0.5 M HCl was prepared and added to a beaker containing 13.7 mg of 4-aminobenzoic acid and 6.9 mg of sodium nitrite. After 30 min agitation under a nitrogen atmosphere, the diazonium salt of 4-aminobenzoic acid was obtained (Fig. 1). The same procedure was done with 0.25 M H_2SO_4.

The product obtained was characterized by Fourier transform infrared (FTIR) spectroscopy. The FTIR spectrum (Fig. 1S†) was recorded using the Nicolet iS10 FTIR spectrometer (Thermo Scientific) *via* the Attenuated total reflection (ATR) technique, covering the range from 2350 cm^{-1} to 600 cm^{-1} and allowed for the evidence of characteristic functional groups including the diazo group N≡N and C–N bond which appeared at 2292 cm^{-1} and 1212 cm^{-1}, respectively.[18]

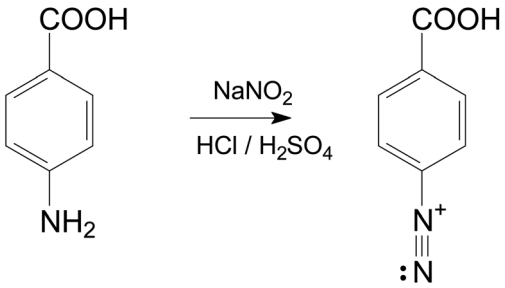

Fig. 1 Chemical synthesis of 4-carboxyphenyl diazonium.

2.3. Electrochemical experiments

Before each experiment, the MS surface, used as a working electrode, was mechanically cleaned using emery paper with different grit sizes, including 350, 500, and 1200. Afterwards, MS surface was rinsed in acetone and thoroughly with double distilled water. A platinum sheet (2 cm^2 surface area) was used as a counter electrode. All potentials were reported *versus* a Ag/AgCl (3.5 M KCl) reference electrode. All measurements were carried out using a Potentiostat/Galvanostat CHI660D electrochemical workstation, and each measurement was repeated at least three times.

For the electrografting, three successive cyclic voltammograms were recorded in 0.5 M HCl or 0.25 M H_2SO_4 containing 2 mM diazonium salt. During each measurement, the working electrode (MS) was reduced and oxidized electrochemically by sweeping the applied electrode potential from +0.60 V to −0.60 $V_{Ag/AgCl}$ and back at 100 mV s^{-1} potential scan rate. After modification, the electrode was thoroughly rinsed with either 0.5 M HCl or 0.25 M H_2SO_4. Electrochemical impedance spectroscopy (EIS) measurements were conducted between 10^4 Hz and 10^{-2} Hz with an amplitude of 5.0 mV. The impedance results obtained were represented using both Nyquist and Bode plots, and a simple equivalent Randles CPE circuit (Fig. 2S†) was used to fit impedance data and extract the polarization resistance (R_p). The following equation was then used to calculate the inhibition efficiency (IE%):

$$IE\% = \left(\frac{R_{p(i)} - R_{p(o)}}{R_{p(i)}}\right) \times 100 \quad (1)$$

where $R_{p(i)}$ and $R_{p(o)}$ are the inhibited and uninhibited polarization resistance, respectively.

The potentiodynamic polarization measurements were performed by scanning from open circuit potential (E_{OCP}) either towards cathodic or anodic potentials at 1.0 mV s^{-1}. Corrosion current density (i_{corr}) was obtained by extrapolating the linear points at around ±50 mV, and/or within a current range of about 10 factor, of the open circuit potential with the log *i* axis. The inhibition efficiency was calculated using the following equation:

$$IE\% = \left(\frac{i_{corr(o)} - i_{corr(i)}}{i_{corr(o)}}\right) \quad (2)$$

where $i_{corr(o)}$ and $i_{corr(i)}$ are the corrosion current density of MS without and with the inhibitor, respectively.

During these measurements, a magnetic stirrer was used to stir the solution at 100 rpm. The electrodes (working, reference and counter) were arranged in a triangle with the reference electrode located near the working electrode. The stirring bar was positioned about 2 cm above the working electrode surface.

Before performing EIS and potentiodynamic polarization experiments, E_{OCP} was examined for 1800 s in order to reach a steady state on the MS surface. All experiments were performed at room temperature.

The inhibition efficiency was estimated using corrosion current density (i_{corr}) and the polarization resistance (R_p) of the studied system.

2.4. Surface characterization

The changes occurring on MS surface in the presence and the absence of diazonium salt were monitored by examining the morphology and the composition of the substrate using Field Emission Scanning Electron Microscopy coupled with Energy Dispersion X-ray (FESEM-EDX). FESEM-EDX was performed with an ultra-high resolution scanning electron microscope Quanta 650 Field Emission and Energy Dispersion X-ray Spectrometer. The wettability of MS surface was characterized by contact angle measurement of water using a Theta Lite optical tensiometer (Biolin Scientific).

2.5. Theoretical calculations

Gaussian 09W software was used to perform the quantum theoretical calculations. Based on the density functional theory (DFT), the basis set 6-311 ++G(d,p) and the hybrid functional B3LYP were selected for this study. Some electronic parameters, such as the energy of the highest occupied molecular orbital (E_{HOMO}), the energy of the lowest unoccupied molecular orbital (E_{LUMO}), the energy gap (ΔE) between LUMO and HOMO and Mulliken charges on the backbones atoms, were determined. The optimized molecular structures and HOMO surfaces were visualized.

3. Results and discussion

3.1. Electrochemical impedance spectroscopy measurements

This study was performed to investigate the modification occurring on MS surface while diazonium salt of 4-aminobenzoic acid (4-ABA) was attached through electrografting or spontaneous grafting in acidic solutions. Fig. 2a and b show the Nyquist diagrams of MS surface in 0.5 M HCl and 0.25 M H_2SO_4 containing diazonium salt of 4-ABA. Without any modification of MS surface, one can observe a typical suppressed semi-circle with R_p of 21.2 Ω cm^2 in 0.5 M HCl (black curve in Fig. 2a) and 23.6 Ω cm^2 in 0.25 M H_2SO_4 (black curve in Fig. 2b). After electrografting of diazonium salt (red curves in Fig. 2), one can observe approx. a 3-times and 2-times increase of the polarization resistance in 0.5 M HCl and 0.25 M H_2SO_4, respectively. Elsewhere, Nyquists plots of MS surfaces without and with electrochemical assistance in either HCl or H_2SO_4 without the inhibitor reveal no change of the polarization resistance (as

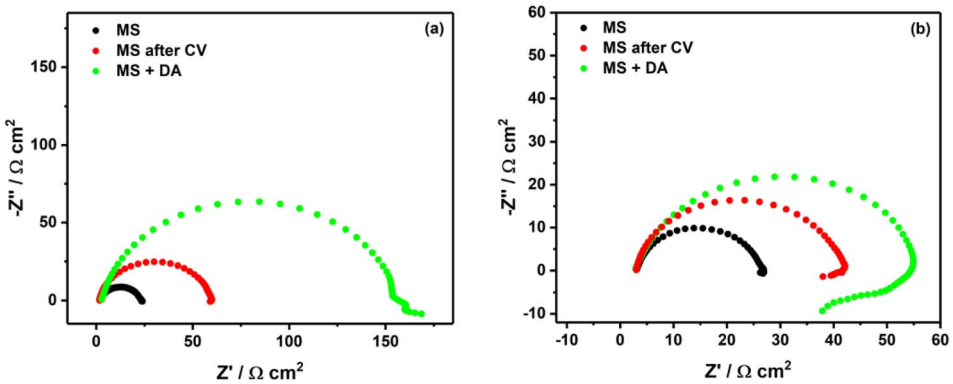

Fig. 2 Nyquist plots of unmodified and modified MS surface in (a) 0.5 M HCl and (b) 0.25 M H_2SO_4. DA for diazonium, CV for cyclic voltammetry.

Table 1 Polarization resistance, corrosion current density and inhibition efficiency (calculated using corrosion current density) of bare MS and modified MS by with and without electrochemical assistance[a]

	R_p (Ω cm^2)	E_{corr} (mV per Ag/AgCl)	i_{corr} (10^{-10} A cm^{-2})	IE%
MS in HCl	21.2	−473	127.9	
MS in H_2SO_4	23.6	−491	160.3	
MS electrografted in HCl	57.7	−450	29.2	77.2
MS electrografted in H_2SO_4	38.9	−466	69.8	56.5
MS in HCl + DA	153.7	−450	2.1	98.4
MS in H_2SO_4 + DA	53.1	−443	ND	ND

[a] ND not determined IE inhibition efficiency.

shown in Fig. 3S†). This confirms that the observed increase in the polarization resistance is attributed to the protective effect of the electrografted diazonium on the MS surface. This observation is consistent with the previous research conducted by Pinson's group, which also showed a similar trend using more complex diazonium salts.[15,16]

Furthermore, when MS surface was left in the corrosion medium in the presence of the diazonium salt, a significant increase of the polarization resistance was observed (green curves in Fig. 2). Such increase is more pronounced in 0.5 M HCl (about 7 times), and less than 3 times in 0.25 M H_2SO_4 (Table 1).

Given that MS has a positive charge in acidic media,[11] a possible explanation of the good inhibition performance in HCl can be attributed to the adsorption of chlorides in the inner Helmholtz plane (IHP) of MS surface. Thereby more diazonium molecules move to the electrode surface *via* electrostatic attraction of chlorides. Conversely, due to their size, sulfates are more present in the outer Helmholtz plane (OHP), resulting in less diazonium molecules being electrostatically attracted. Thus, in addition to the electrografting or spontaneous grafting of diazonium molecules, in the case of HCl there is an additional electrostatic force conveying more diazonium molecules to the MS surface.

In both solutions, the impedance spectra exhibit a single capacitive loop at high frequencies, while at low frequencies there is an additional small inductive loop in 0.25 M H_2SO_4. The single capacitive loop at high frequencies is usually attributed to the polarization resistance (R_p), while the small inductive loop observed with sulfuric acid is related to the relaxation process, probably due to the low surface coverage of diazonium salt.[13,14] Furthermore, the depression of the semi-circles observed in both acidic solutions can be most likely explained by the heterogeneity of the MS surface.[11,14]

In the Bode plots (Fig. 3), we can observe a significant increase of log Z when the MS surface is in the corrosive solution containing the diazonium salt (green curves).

In Fig. 3b, one can better observe a deviation of log Z at low frequencies (green curves), which confirms the detachment of some diazonium molecules from the MS surface in H_2SO_4. log Z is steadier at low frequencies when MS surface is electrografted in H_2SO_4 (Fig. 3b, red curves). This might reveal a better stability of the film formed *via* electrografting.

3.2. Stability of the inhibition film

In the literature, Pinson group is the one which has investigated the most grafting of diazonium salt on iron and MS.[15–19] Surprisingly, in any of their studies the stability of the film formed through grafting of the diazonium salt was scrutinized. They have noticed that less than 1 h is needed for the organic layer formation on MS surface, and that after 1 h immersion of

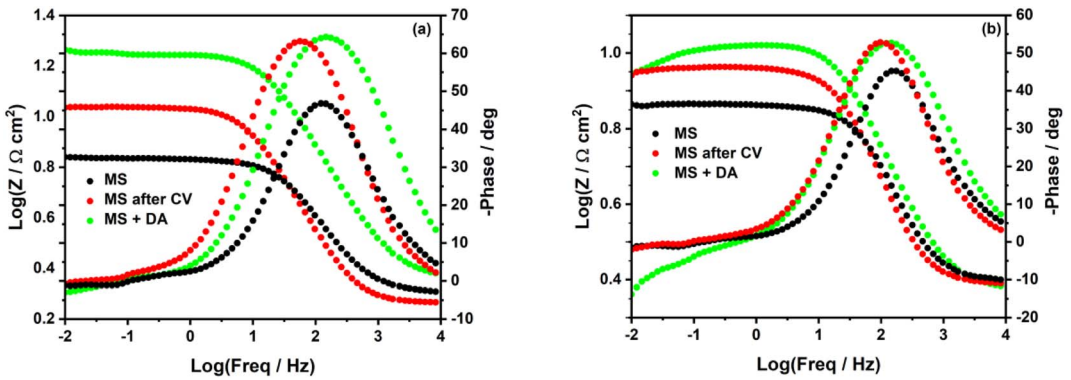

Fig. 3 Bode plots of unmodified and modified mild steel surface in (a) 0.5 M HCl and (b) 0.25 M H_2SO_4.

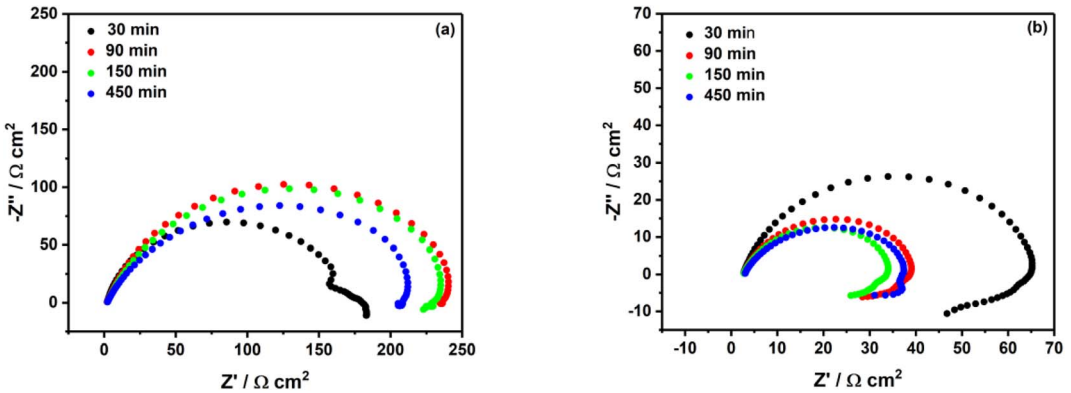

Fig. 4 Nyquist plots of mild steel surface in (a) 0.5 M HCl and (b) 0.25 M H_2SO_4 containing 2 mM diazonium salt at different immersion times.

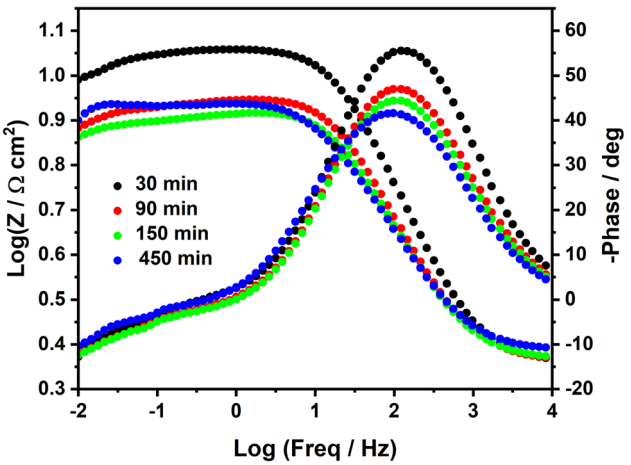

Fig. 5 Bode plots of MS surface in 0.25 M H_2SO_4 containing 2 mM diazonium salt at different immersion times.

iron in the grafting solution the inhibition efficiency did not change significantly.[17,18] In the present study, the immersion time of MS surface in acidic solutions containing 2 mM diazonium salt was investigated. It comes out that after a 90 min immersion in 0.5 M HCl, one can observe an increase of the R_p (approx. 92% of the inhibition efficiency, see the red curve in Fig. 4a). However, for longer immersion times, the inhibition efficiency decreases, as highlighted by the decrease in the R_p (green and blue curves in Fig. 4a).

In sulfuric acid solution, the stability behavior looks different. The largest semi-circle diameter was recorded after 30 min of immersion (black curve in Fig. 4b), and one can notice a significant decrease of the inhibition efficiency (30%) after 90 min, 150 min and 450 min. Most likely the film formed in sulfuric acid is less stable compared to the film formed in hydrochloric acid.

Such poor stability of the diazonium film in sulfuric acid solution is well highlighted in the Bode plots (Fig. 5), where we can observe a systematic decrease of log Z at low frequencies. In agreement with earlier studies,[17,18] a short time, such as 90 min in HCl and 30 min in H_2SO_4, was needed to obtain a good inhibition efficiency.

3.3. Polarization curves of modified MS surface

Fig. 6 shows the semi-logarithmic polarization curves for unmodified, electrografted and spontaneous grafted MS surface with a diazonium salt in HCl (Fig. 6a) and H_2SO_4 (Fig. 6b).

In 0.5 M HCl, polarization curves exhibit a decrease in the i_{corr} by 77.2% and 98.4% for MS surface electrografted and spontaneous grafted, respectively (Table 1). Regarding the corrosion potential, one can observe a shift of 23 mV towards anodic potentials for both MS modifications. In 0.25 M H_2SO_4, in consistence with Nyquist behavior, we can observe a poor decrease in the corrosion current density for MS electrografted and spontaneous grafted. Concomitantly, we can observe a shift of the corrosion potential towards anodic values of 25 mV and 48 mV for MS electrografted and spontaneous grafted, respectively. In general, the shift of corrosion potential towards anodic values reveals that the organic layer formed is an anodic inhibitor. Nonetheless, even though the trend of inhibition is the same in both acidic media, the values of the inhibition efficiency obtained from corrosion current density are higher than the values obtained from the polarization resistance curves. A similar shift towards positive potentials was obtained after the electrografting of stainless steel with the diazonium salt of 4-aminobenzylphosphonic acid.[20]

3.4. Scanning electron microscopy coupled with energy dispersive X-ray spectroscopy (SEM-EDX)

SEM-EDX was used as additional technique to learn about the morphology and elemental composition of the layer formed on the mild steel surface before and after exposure to the corrosive solutions, with and without the diazonium salt grafting. Fig. 7 shows SEM images of MS surfaces exposed to acid solutions (Fig. 7b–d) and acid solutions containing 2 mM diazonium salt (Fig. 7c–e) for 12 h. One can observe that without the diazonium salt the surface of MS was severely corroded with porous-like structures and loss of electrode material (see Fig. 7b and d). However, the loss of electrode material seems more pronounced in sulfuric acid, with formation of smaller pores (Fig. 7d).

In the presence of diazonium salt, one can observe a protective layer containing long cracking lines in 0.25 M H_2SO_4 (Fig. 7e) and look smoother in 0.5 M HCl (Fig. 7c). These cracking lines may be

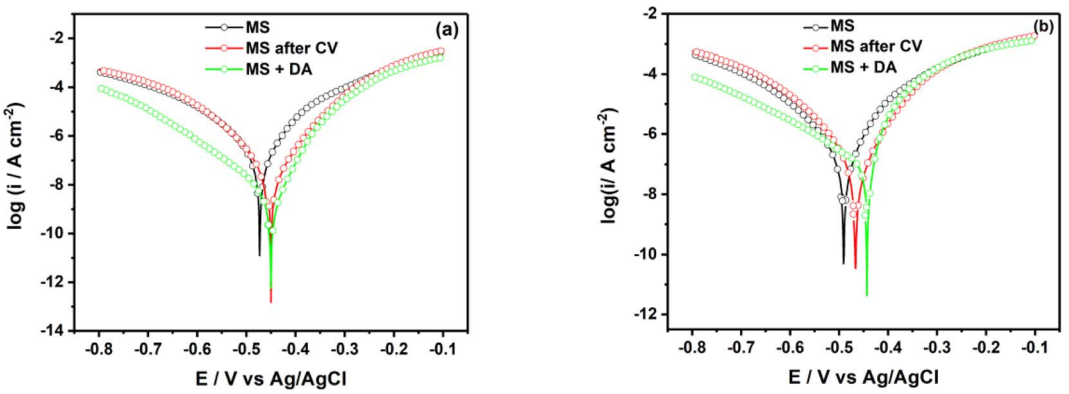

Fig. 6 Logarithmic polarization curves of mild steel surface in (a) 0.5 M HCl and (b) 0.25 M H_2SO_4 containing 2 mM diazonium salt.

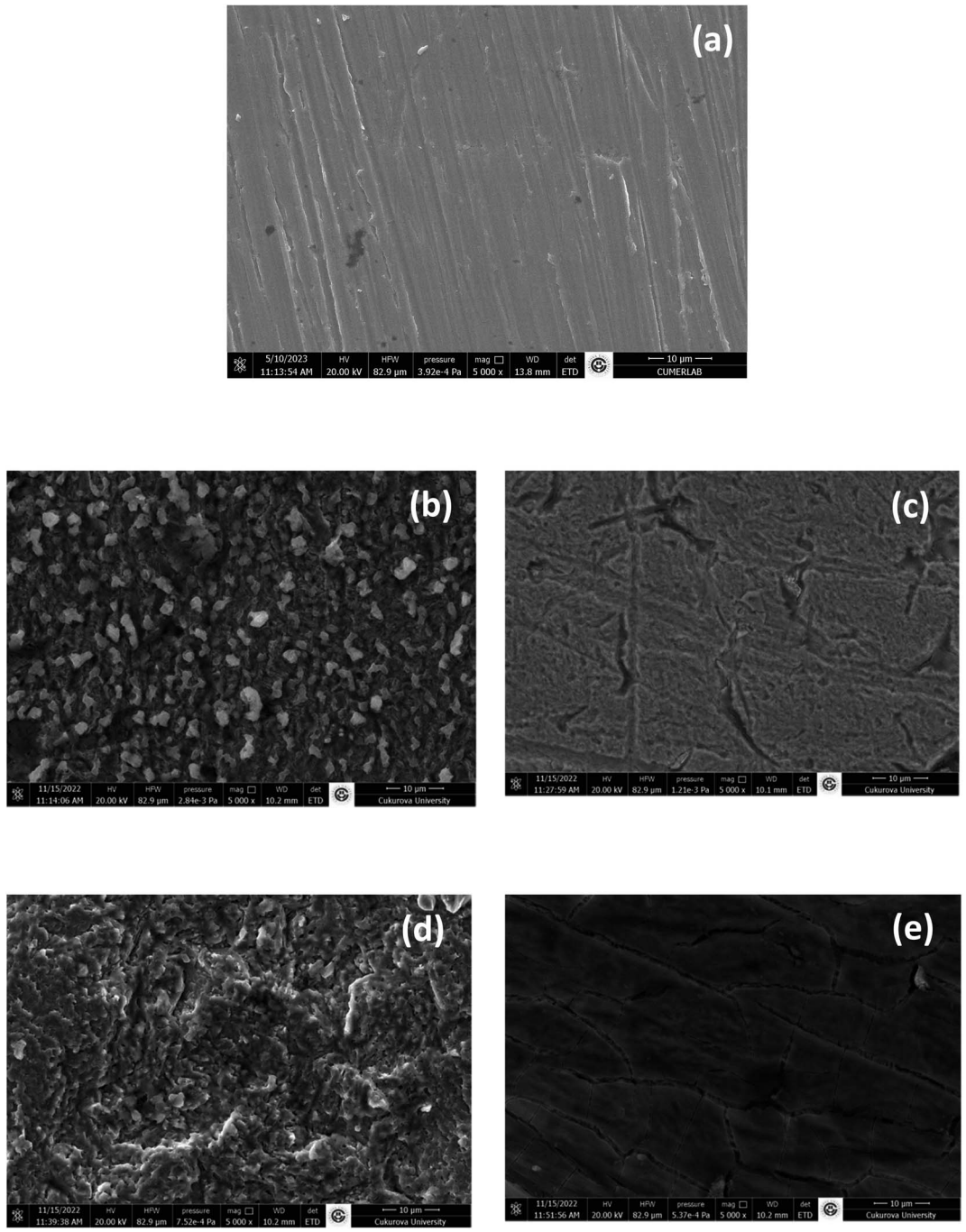

Fig. 7 SEM images of mild steel surfaces before (a) and after immersion for 12 h at room temperature in (b and c) 0.5 M HCl and (d and e) 0.25 M H_2SO_4 solutions, (b and d) in the absence and (c and e) in the presence of 2 mM diazonium salt.

the weakness of this film because as noticed previously inhibition efficiency is poor in sulfuric acid solution.

In Table 2, elemental analysis of MS surface without diazonium salt reveals a smaller percentage of carbon in either 0.5 M HCl and 0.25 M H_2SO_4. This percentage is attributed to the inherent composition of MS material, the largest percentage being for iron. In the presence of the diazonium salt, the increased percentage of carbon reveals the formation of the organic layer on the mild steel surface. The benzene ring and the carboxylic group most likely contributed to such percentage increase.

Table 2 Percentage of elements for each specimen obtained from the energy dispersive X-ray spectroscopy (EDX) analysis after 12 h immersion in either 0.5 M HCl or 0.25 M H_2SO_4, in the presence or absence of 2 mM diazonium salt

	Element (weight%)			
Sample	C	N	O	Fe
MS in HCl	3.5	1.1	5.1	86.4
MS in HCl + DA	30.1	1.2	6.7	60.2
MS in H_2SO_4	2.2	1.4	39.1	40.3
MS in H_2SO_4 + DA	40.8	1.8	11.1	45.1

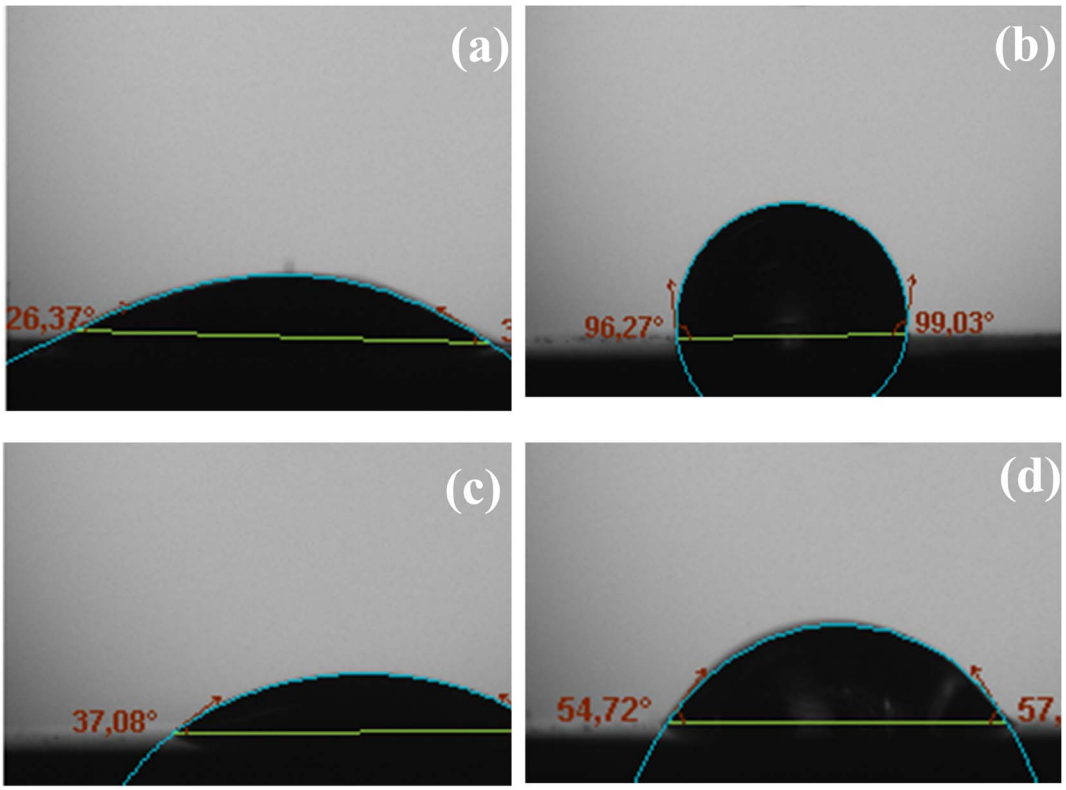

Fig. 8 Contact angles of drop of distilled water on mild steel surfaces recorded after immersion for 2 h at room temperature in (a and b) 0.5 M HCl and (c and d) 0.25 M H_2SO_4 solutions, (a and c) in the absence and (b and d) in the presence of 2 mM diazonium salt.

The measured contact angles (Fig. 8) for the MS surface in the presence and the absence of the diazonium salt strongly validated the presence of a layer exhibiting essentially a hydrophobic property from which anticorrosion efficiency derived.

Definitely, there is a noteworthy correlation of this result with SEM images obtained with mild steel surface immersed in 0.5 M HCl and in 0.25 M H_2SO_4.

3.5. Insights according to the density functional theory (DFT)

For the reaction of diazonium salts on metallic surfaces, three species such as diazonium salt itself, radical and carbocation (obtained from the heterolytic or homolytic dediazonation) are usually evoked in the mechanism scheme.[21–23] In this study, we will emphasize on the diazonium molecule. As shown in Fig. 9, the structure of 4-carboxyphenyldiazonium salt was optimized, the distribution of electron clouds and its energy value, electrostatic potential map and dipoles moments were calculated.

One can observe that the molecule has delocalized π-electrons in its benzene cycle and in the branch containing diazonium (Fig. 9, left). The highest Mulliken charge is on oxygen (−0.310), followed by the first nitrogen (−0.300). In the literature, it is well known that the highest occupied molecular orbital (HOMO) describes molecular sites accountable for

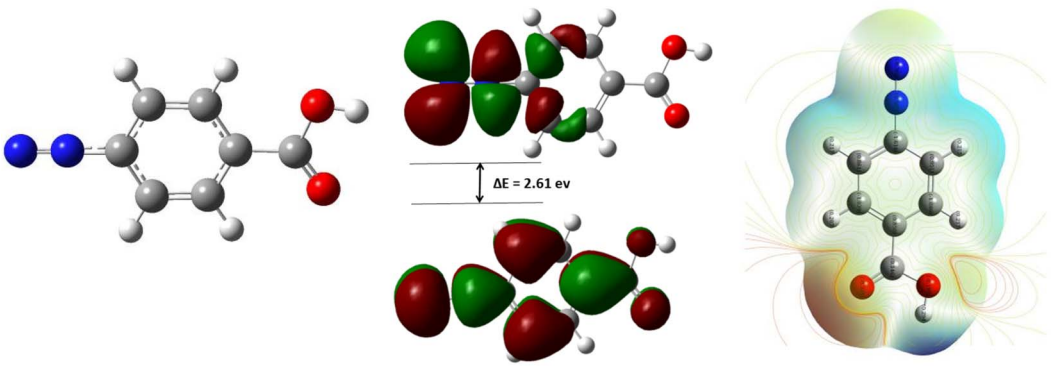

Fig. 9 Optimized molecular structure (left), HOMO (middle down) and LUMO (middle up) orbitals, Mulliken charges, surface and contours maps (right) of the electrostatic potential (ESP) on electron density surface of 4-carboxybenzenediazonium salt.

electron transfer and the lowest unoccupied molecular orbital (LUMO) is for electron acceptance.[24–26] Looking at HOMO and LUMO, one can easily see that the reaction is located mainly on the diazonium group (HOMO and LUMO electron density) and on the aromatic site (HOMO). These moieties of the molecule are most likely involved in the interaction with the surface of iron *via* donation and back-donation of electrons on those sites. Furthermore, the small energy gap between LUMO and HOMO ($\Delta E = 2.61$ eV) indicates a good reactivity of the molecule and thus its strong interaction with MS surface.[24,26] These molecular insights correlate with the good corrosion inhibition efficiency obtained from experimental studies.

4. Conclusions

In this study, we explored the modification of MS surface using both electrografting and spontaneous grafting of 4-carboxyphenyl diazonium in acidic solutions. The modification successfully incorporated the diazonium as a corrosion inhibitor. After the modification, it was found out that MS surface in the presence of diazonium, exhibited different impedance trends in HCl and H_2SO_4. In the former solution, the inhibition efficiency was higher (86%) and in the later solution, the detachment of diazonium molecules was envisaged. This discrepancy between the acidic solutions comes from their respective anions chlorides and sulfates which acquired different localization around the vicinity of the MS surface. The study of the stability revealed that the film formed on the MS surface exhibits poor stability for a long time (after 90 min and 30 min in 0.5 M HCl and 0.25 M H_2SO_4, respectively). SEM images reveal that the structure of the film formed in HCl containing diazonium salt is smoother with less crack lines. The small energy gap value matches with the good corrosion inhibition efficiency of 4-carboxyphenyl diazonium.

Conflicts of interest

There are no conflicts to declare.

Acknowledgements

The authors are greatly thankful to Çukurova University Research Fund for financial support. PMST acknowledges Dr Marta Meneghello (Postdoc, Université de Bordeaux, France) for her help in the proofreading of the paper.

References

1 G. Koch, J. Varney, N. Thompson, O. Moghissi, M. Gould and J. Payer, International measures of prevention, application, and economics of corrosion technologies study, in *NACE International IMPACT Study*, NACE International, Houston, 2016, https://impact.nace.org/documents/Nace-International-Report.pdf.

2 Y. D. V. Yasuda, F. A. M. Cappabianco, L. E. G. Martins and J. A. B. Gripp, *Comput. Ind.*, 2022, **141**, 103695.

3 S. Vishnuvardhan, A. R. Murthy and A. Choudhary, *Int. J. Pressure Vessels Piping*, 2023, **201**, 104853.

4 S. Sharma and A. Kumar, *J. Mol. Liq.*, 2021, **322**, 114862.

5 S. Z. Salleh, A. H. Yusoff, S. K. Zakaria, M. A. A. Taib, A. A. Seman, M. N. Masri, M. Mohamad, S. Mamat, S. A. Sobri, A. Ali and P. T. Teo, *J. Cleaner Prod.*, 2021, **304**, 127030.

6 M. A. El-Hashemy, A. E. Hughes, T. Gengenbach, A. M. Glenn and I. S. Cole, *J. Rare Earths*, 2023, **41**, 309.

7 J. Tan, L. Guo, H. Yang, F. Zhang and Y. El Bakri, *RSC Adv.*, 2020, **10**, 15163.

8 B. Židov, Z. Lin, I. Stojanović and L. Xu, *J. Appl. Polym. Sci.*, 2021, **138**, e49614.

9 G. Kordas, *Corros. Mater. Degrad.*, 2022, **3**, 376.

10 H. Hossini, B. Shafie, A. D. Niri, M. Nazari, A. J. Esfahlan, M. Ahmadpour, Z. Nazmara, M. Ahmadimanesh, P. Makhdoumi, N. Mirzaei and E. Hoseinzadeh, *Environ. Sci. Pollut. Res.*, 2022, **29**, 70686.

11 A. Döner, R. Solmaz, M. Özcan and G. Kardas, *Corros. Sci.*, 2011, **53**, 2902.

12 B. Ngoune, M. Pengou, A. M. Nouteza, C. P. Nanseu-Njiki and E. Ngameni, *ACS Omega*, 2019, **4**, 9081.

13 J. Lazrak, E. Ech-chihbi, R. Salim, T. Saffaj, Z. Rais and M. Taleb, *Colloids Surf., A*, 2023, **664**, 131148.

14 R. Hsissou, K. Dahmani, A. E. Magri, A. Hmada, Z. Safi, N. Dkhireche, M. Galai, N. Wazzan and A. Berisha, *Polymers*, 2023, **15**, 1967.

15 A. Adenier, M. Bernard, M. M. Chehimi, E. Cabet-Deliry, B. Desbat, O. Fagebaume, J. Pinson and F. Podvorica, *J. Am. Chem. Soc.*, 2001, **123**, 4541.

16 A. Chaussé, M. M. Chehimi, N. Karsi, J. Pinson, F. Podvorica and C. Vautrin-Ul, *Chem. Mater.*, 2002, **14**, 392.

17 A. Adenier, E. Cabet-Deliry, A. Chaussé, S. Griveau, F. Mercier, J. Pinson and C. Vautrin-Ul, *Chem. Mater.*, 2005, **17**, 491.

18 C. Combellas, M. Delamar, F. Kanoufi, J. Pinson and F. I. Podvorica, *Chem. Mater.*, 2005, **17**, 3968.

19 A. Berisha, C. Combellas, F. Kanoufi, J. Pinson and F. I. Podvorica, *Electrochim. Acta*, 2011, **56**, 10762.

20 X. T. Le, G. Zeb, P. Jégou and T. Berthelot, *Electrochim. Acta*, 2012, **71**, 66.

21 K. Boukerma, M. M. Chehimi, J. Pinson and C. Blomfield, *Langmuir*, 2003, **19**, 6333.

22 S. Betelu, I. Tijunelyte, L. Boubekeur-Lecaque, I. Ignatiadis, J. Ibrahim, S. Gaboreau, C. Berho, T. Toury, E. Guenin, N. Lidgi-Guigui, N. Félidj, E. Rinnert and M. Lamy de la Chapelle, *J. Phys. Chem. C*, 2016, **120**, 18158.

23 A. Berisha, C. Combellas, F. Kanoufi, P. Decorse, N. Oturan, J. Médard, M. Seydou, F. Maurel and J. Pinson, *Langmuir*, 2017, **33**, 8730.

24 A. O. Yüce, B. D. Mert, G. Kardas and B. Yazıcı, *Corros. Sci.*, 2014, **83**, 310.

25 A. Keleşoğlu, G. Sığırcık, R. Yıldız and İ. Dehri, *J. Dispersion Sci. Technol.*, 2021, **44**, 329.

26 H. S. Sujatha and M. Lavanya, *Can. Metall. Q.*, 2022, **1**, DOI: 10.1080/00084433.2022.2140398.